Selective alkylation by photogenerated aryl and vinyl cation

Slegt, Micha

Chapter 2 | **Photochemistry of para-substituted diphenyliodonium salts**

Introduction

The first publication concerning diphenyliodonium salts appeared in 1894 and reported their preparation[1]. This paper elaborated on even earlier work on the preparation of λ_3-iodane (hypervalent iodonium) compounds[2]. The methods of synthesis of these compounds and their applications in other syntheses have since continuously developed[3]. The photolability of iodonium salts was first noted in the late 1950's[4,5] which eventually led to extensive use of these salts in both negative and positive photoresists, in industries applying photolithography, such as computer-chip manufacturers[6].

Over 130 patents and over 50 scientific publications have appeared mainly dealing with alterations of the diphenyliodonium salts' basic structure, mostly to serve specific industrial applications. Lately, the industrial application of diphenyliodonium salts receives competition from the triphenylsulfonium salts[7]. The photochemistry of sulfonium salts, however, takes place along the same lines as the photochemistry of diphenyliodonium salts[8,9].

The industrial applications spurred research on the mechanism of photolysis of diphenyliodonium salts. The first flash photolysis experiments recognised the presence of the radical cation of iodobenzene[10], and since the publication of that finding homolysis of the C-I bond has been considered a major, if not the major mechanistic pathway[11,12,13,14]. In 1990 a mechanism was

Scheme 1: The mechanism of photolysis of diphenyliodonium salts[16].

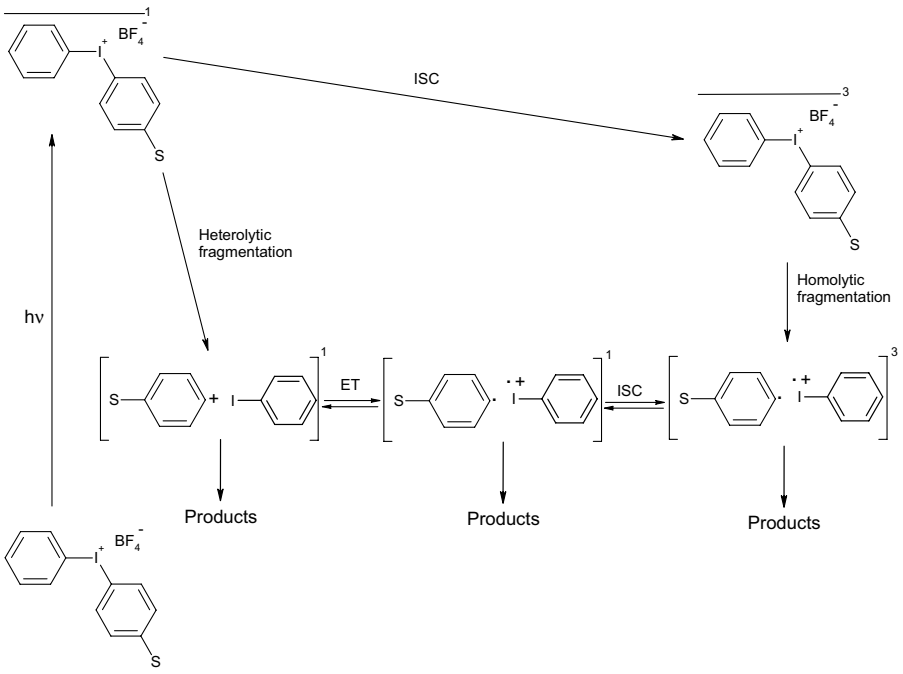

proposed that today still is regarded to be the golden standard for these reactions (Scheme 1)[15,16]. According to that mechanism the photolysis proceeds through heterolysis of the C-I$^+$ bond in the singlet excited state, which produces a phenyl cation-iodobenzene pair, and homolysis of the C-I$^+$ bond in the triplet excited state, which forms a phenyl radical-iodobenzene radical cation pair[16]. Both C-I bonds are prone to heterolysis and homolysis. The available information allows no conclusion about the feasibility of interconversion of the two pairs, nevertheless this process is thought to occur[17].

The intermediacy of phenyl cations [18] in the photolysis of diphenyliodonium salts renews the interest in (the mechanism of) the photolysis of these salts. The photochemical generation of singlet phenyl cations, and even more so of triplet phenyl cations (Figure 1), is a fast-moving area of research these days[19,20].

Figure 1: Singlet and triplet phenyl cations.

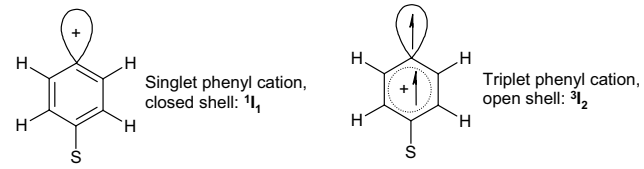

The reported chemoselectivity of triplet (open-shell) phenyl cations compared to fairly un - selective singlet (closed shell) phenyl cations may offer a compromise between a hyper-reactive species and a desired selectivity of action. In this chapter investigations are reported about the photogeneration of phenyl cations from the series of *para*-substituted diphenyliodonium salts **1**-**8** (Chart 1). The compounds were photolyzed in methanol and in acetonitrile in the pres - ence of anisole to probe the reactivity of the product-forming intermediates as a function of the substituent.

Chart 1: Compounds studied.

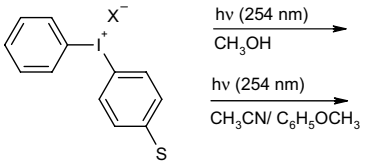

1) S = H, X = BF_4^-
2) S = CH_3, X = BF_4^-
3) S = OCH_2CH_3, X = BF_4^-
4) S = CF_3, X = BF_4^-
5) S = $C(O)OCH_3$, X = BF_4^-
6) S = CN, X = BF_4^-
7) S = $C(O)CH_3$, X = BF_4^-
8) S = $N(CH_3)_2$, X = Br^-

Results and discussion

Syntheses

Six of the *para*-substituted phenyl(phenyl)iodonium tetrafluoroborates studied (**1**-**4**, **6** and **7**) are synthesised by treating the corresponding aryl boronic acids with an equimolar amount of (diacetoxy)iodobenzene in the presence of two mole equivalents of hydrogen tetrafluoroborate (in diethyl ether) at -30° C in dichloromethane, following a modified literature procedure[21,22]. Iodonium salt **5** is prepared from 4-(diacetoxy)iodobenzoic acid methyl ester and phenylbo - ronic acid following the same procedure as for **1**-**4**, **6** and **7**. Compound **8** as tetrafluoroborate salt is not stable and therefore the bromide salt was prepared from 4-N,N-dimethylamino - benzene boronic acid and Koser's reagent, hydroxy(tosyloxy)iodobenzene, (1/1 mole/mole), in tetrahydrofuran at melting ice temperature, followed by tosylate/ bromide anion exchange.

*Photolyses of **1**-**8** in methanol*

Both the phenyl-iodonium bond A and the phenyl-iodonium bond B of the *para*-substituted diphenyliodonium salts **2**-**8** are photolabile (Scheme 2). Heterolytic or homolytic fission of

Scheme 2: Product formation upon irradiation of **1**-**8** in methanol.

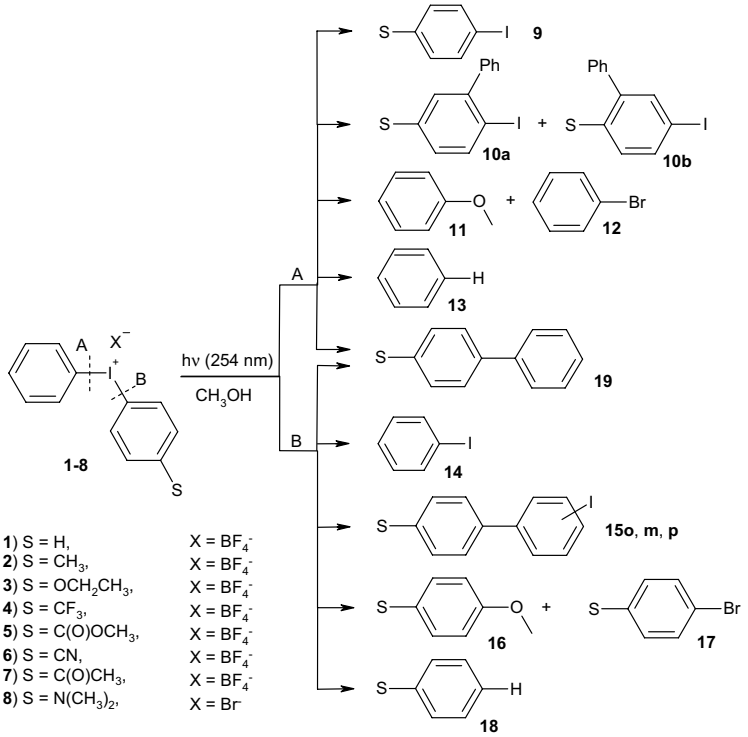

either bond results in the formation of four types of products. Upon A bond cleavage, apart from the leaving group **9**, the Friedel-Crafts type products **10a** and **10b**, the nucleophilic substitution products with the solvent **11** and the counter-ion **12**, and the reductive dehalogenation products **13** are produced. Upon cleavage of bond B, also a leaving group **14** forms, next to the Friedel-Crafts products **15*o***, ***m***, ***p***, the nucleophilic substitution products, with the solvent (**16**), and the counter-ion (**17**), and the reduction products **18**. One product, the *ipso*-substitution Friedel-Crafts product **19**, can be produced through either A or B bond cleavage.

The composition of the product mixtures observed in the photolyses of **1**-**8** in methanol, at low conversion, is recorded in Table 1. Various effects of the substituents are immediately clear. The Friedel-Crafts type products **10a** and **10b** are formed only in the photolyses of **2** (S = CH_3) and **3** (S = OCH_2CH_3) and products **15** only in the irradiation of **1** (S = H); with **2**-**8** at best traces of products **15** are observed (*vide infra*). The formation of ethers **11** and **16** also shows a remarkable substituent effect. Whereas A bond cleavage produces ether **11** in all cases, B bond cleavage only yields ethers **16** in the case of the photolyses of **1**, **2**, **3** and **4** (S = CF_3). Nucleophilic substitution products with the counter-ion, **12** and **17**, are only found in the photolysis of **8**. The reduction products **13** and **18** occur in all experiments. The *ipso*-substitution Friedel-Crafts type products **19** are also generally encountered, but in the photolysis of **1**-**4** about twice as much of these products is formed as in the photolyses of **5**-**8**.

Table 1: Results of the photolyses of **1**-**8** in methanol[a,e].

	S	9	10a,b	11	12	13	14	15	16	17	18	19
1	H	5.8		1.9		1.6	5.8	3.4	1.9		1.6	1.2
2	CH_3	5.1	3.9[b]	1.3		1.3	4.3	[d]	1.6		1.2	1.0
3	OCH_2CH_3	5.6	2.1[c]	0.8		1.4	4.8	[d]	0.3		2.3	1.4
4	CF_3	9.1		2.5		2.0	8.3	[d]	0.4		5.6	1.1
5	$C(O)OCH_3$	3.8		1.9		1.3	5.6	[d]			3.8	0.5
6	CN	3.3		2.7		1.6	6.7	[d]			5.0	0.5
7	$C(O)CH_3$	2.7		1.7		1.5	5.9	[d]			2.6	0.6
8	$N(CH_3)_2$	6.7		0.3	0.4	2.9	11.6	[d]		3.6	1.6	0.7

[a] Percentages of product, relative to internal standard (GC), after 90 minutes of irradiation. [b] Ratio of **10a**: **10b** is 11:1. [c] Ratio of **10a**: **10b** is 2.1:1. [d] Formed in trace amounts, observed after evaporation of the solvent (*o*, *m*, *p* ratios in Table 4). [e] Under the reaction conditions used for the photolysis experiments, except for the light **1**-**8** are inert.

*Photolyses of **1**-**8** in acetonitrile/ anisole 1/1*

Under these conditions the same types of products can be formed as in methanol (cf. Scheme 2). The presence of the extra nucleophile anisole, however, does open an additional product-forming pathway: substitution with this substrate yielding methoxybiphenyls **20** upon A bond cleavage and 4'-substituted-methoxybiphenyls **21** upon B bond fission (Scheme 3).

Scheme 3: Additional products in the photolyses of **1**-**8** in acetonitrile/ anisole (compared to in methanol).

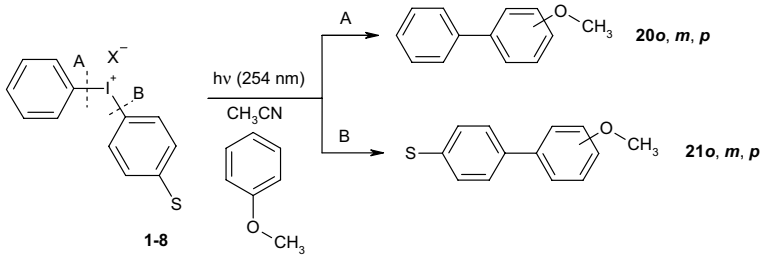

The composition of the product mixtures upon photolysis of **1**-**8** in acetonitrile/ anisole is recorded in Table 2. The Friedel-Crafts arylation of anisole yielding **20** and **21** is the major product-forming pathway upon both A and B bond fission; the Friedel-Crafts products **10**, **15** and **19** are formed in negligible amounts compared to **20** and **21**. No products of the nucleophilic substitution reaction with acetonitrile (acetanilides, formed through a Ritter reaction) are found. Nucleophilic substitution products with the counter-ion (**12** and **17**) are produced only in the irradiation of **8**. The reduction products **13** and **18** are formed in every experiment in this series.

Table 2: Results of the photolyses of **1**-**8** in acetonitrile/ anisole[a,b].

	S	9	12	13	20	14	17	18	21	20*o*:*m*:*p*	21*o*:*m*:*p*
1	H	20.8		6.9	27.1	20.8		6.9	27.1	69:11:20	69:11:20
2	CH_3	27.1		7.2	25.1	18.5		11.0	20.7	71:11:18	73:11:16
3	OCH_2CH_3	20.7		5.5	22.3	17.9		7.8	17.9	66:11:23	74:11:15
4	CF_3	19.8		5.7	19.1	24.3		5.6	45.2	70:09:21	71:11:18
5	$C(O)OCH_3$	16.3		5.4	22.1	23.6		4.3	26.8	67:09:24	74:10:16
6	CN	10.9		5.3	22.2	24.7		3.6	36.7	65:10:25	78:08:14
7	$C(O)CH_3$	13.1		5.1	22.4	22.8		4.8	31.2	67:10:23	76:10:14
8	$N(CH_3)_2$	14.2	4.1	5.2	9.6	18.1	12.0	1.1	1.6	77:12:11	100:0:0

[a] Percentages of total product formation (GC) after 90 minutes of irradiation. [b] Under the reaction conditions used for the photolysis experiments, except for the light **1**-**8** are inert.

The *ortho*: *meta*: *para* ratios in which the Friedel-Crafts products **20** and **21** are formed are also presented in Table 2. In general, the percentage of *ortho* isomer is more pronounced upon B bond cleavage, leading to **21**, than upon A bond cleavage, leading to **20**. For the *para* isomer the reverse is true. For both cleavages higher *ortho* yields are connected to lower *para* yields and vice versa.

Except for **8**, the *o*: *m*: *p* ratios in **20** observed upon A bond cleavage are similar: the results of the irradiations of **1**, **2** and **4** are alike, as are the ratios obtained in the photolysis of **3**, **5**, **6** and **7**. The results of the irradiation of **8** also stand out for the B bond fission. No systematic variation in the *o*: *m*: *p* ratios in **21** found upon B bond photocleavage of **2**-**7** is obvious.

Theoretical evaluation of C-I$^+$ bond cleavage pathways

The photochemical bond cleavage pathways of iodonium species have not yet been theoretically evaluated even though this has been done for sulfonium compounds [9], and for onium compounds in general[23].

The diphenyliodonium compound [A-I$^+$-B] is considered as a system consisting of three separate parts, A, I$^+$ and B, connected by two C-I bonds. As with the triphenylsulfonium compounds[9] the thermal dissociation process is expected to result in either [A$^+$ /IB] or [AI /B$^+$] of which the cation-molecule pair of lower energy will be preferred.

To describe the photochemical processes the following orbitals were taken into account: the π and π* orbitals of A (π_A and π_A^*) and B (π_B and π_B^*), the σ bonding and anti-bonding orbitals of A (σ_A and σ_A^*) and B (σ_A and σ_A^*) and a lone pair on iodine (n). The model was refined by taking interaction of the π and σ orbitals into consideration. The relative stabilities of the structures that occur upon elongation of the A-I$^+$ bond from the equilibrium geometry structure (Figure 2) were HF/CEP-121G calculated[24].

Figure 2: Equilibrium geometry of the diphenyliodonium compound.

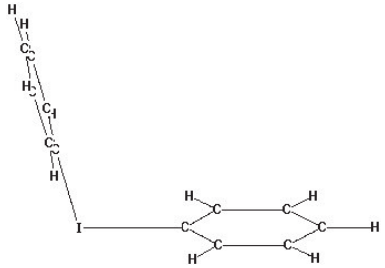

The evaluation reported here indicates eight different intermediate-forming pathways. Electronic excitation of [A-I$^+$-B] may lead to a $\pi_A\pi_A^*$ or a $\pi_B\pi_B^*$ state. A relative preference of π_A^* over π_B^* or *vice versa* will depend on the electron richness of the aromatic rings. These configurations are non-dissociative. However, following the potential energy curve (along the C-I bond elongation) they connect with the dissociative $\sigma\sigma^*$ states in the nearest and in the opposite C-I bond. The $\sigma_A\sigma_A^*$ state correlates with an A•/BI•+ pair and the $\sigma_B\sigma_B^*$ state with a B•/ AI•+ pair. So, in the case of e.g. a $\pi_A \rightarrow \pi_A^*$ excitation an A•/ BI•+ pair may be produced next to a B•/ AI•+ pair.

Also, direct dissociative $\pi \rightarrow \sigma^*$ excitations are possible: $\pi_A \rightarrow \sigma_A^*$, $\pi_A \rightarrow \sigma_B^*$, $\pi_B \rightarrow \sigma_A^*$, and $\pi_B \rightarrow \sigma_B^*$. The $\pi_A\sigma_A^*$ state leads to an $(A^+)^*$/BI ion pair, in which $(A^+)^*$ is the excited state of the phenyl cation (which is an open-shell species). The $\pi_A\sigma_B^*$ and the $\pi_B\sigma_A^*$ states lead to a B•/ AI•+ pair and an A•/BI•+ pair, respectively. The $\pi_B\sigma_B^*$ state leads to a $(B^+)^*$/AI ion pair. Like $(A^+)^*$, $(B^+)^*$ is the excited state of the phenyl cation. If $(A^+)^*$ and $(B^+)^*$ are not sufficiently stabilised by their substituents, or not efficiently trapped, they may convert to their ground state configuration.

Further, excitations to the dissociative $n\sigma^*$ state, of a lone pair on iodine to an anti-bonding σ^* orbital, are possible. They lead to an A•/ BI•+ pair from $n\sigma_A^*$ and a B•/AI•+ pair from $n\sigma_B^*$.

Product-formation may be possible through all 8 channels because energy differences are small. Many of the states are close in energy and may be connected. In particular the $\pi\sigma^* \rightarrow \sigma\sigma^*$ conversion is likely, if both states have a σ^* orbital in common. These processes ($\pi_A\sigma_A^*$ into $\sigma_A\sigma_A^*$, $\pi_A\sigma_B^*$ into $\sigma_B\sigma_B^*$, $\pi_B\sigma_A^*$ into $\sigma_A\sigma_A^*$, and $\pi_B\sigma_B^*$ into $\sigma_B\sigma_B^*$) result in interconversion of the radical pairs or conversion of a ion pair into a radical pair. The conversions are less likely if the fragments are well-separated or stabilised. Solvation upon elongation of the C-I^+ bond and/or stabilisation by means of appropriate substituents may be of decisive influence on the relative stabilities of the possible intermediates.

The presence of an iodine atom induces efficient intersystem crossing which converts a molecule from its singlet excited state into its triplet excited state. For that reason, the photochemistry of diphenyliodonium salts is thought to take place through the triplet excited state. That in these compounds, the iodine is dicoordinated should be of no concern, because the spin-orbit coupling, that causes the intersystem crossing, is only proportional to the atomic number[25].

Substituents on diphenyliodonium salts not only affect the relative stabilities of the fragments of the photoinitiated bond cleavage reactions. They also have more fundamental effects: a) On the energy and the nature of the orbital from which excitation takes place, the highest occupied molecular orbital (HOMO). b) On the efficiency of intersystem crossing (ISC). E.g. the acetyl substituent, that possesses an easily accessible triplet $n\pi^*$ state of its own, at the *para*-position of phenyldiazonium salts, gives efficient ISC and thereby a triplet pathway in product-formation[26,27]. The same effect may be exerted by other carbon-heteroatom double-bond containing substituents.

*Photoreactivity of **1**-**8** in methanol*

The sum of the amounts of leaving groups **9** and **14** as a function of the time of irradiation [28] forms an indication for the progress of the photoreactions (Figure 3). These graphs show that the photoreactivities of **1**-**8** are subject to an unexpected order of substituent effects, not similar to the effects in thermal reactions. In the thermolysis of iodonium compounds the difference

in electron densities in the two C-I bonds, that are modified by substituents on the ring, determines the overall stability[29]. The stability is enhanced by *ortho* and *para* electron-donating substituents. This rationale does not hold for the stability upon irradiation.

Figure 3: The formation of **9** + **14** from **1**-**8** as a function of time of irradiation.

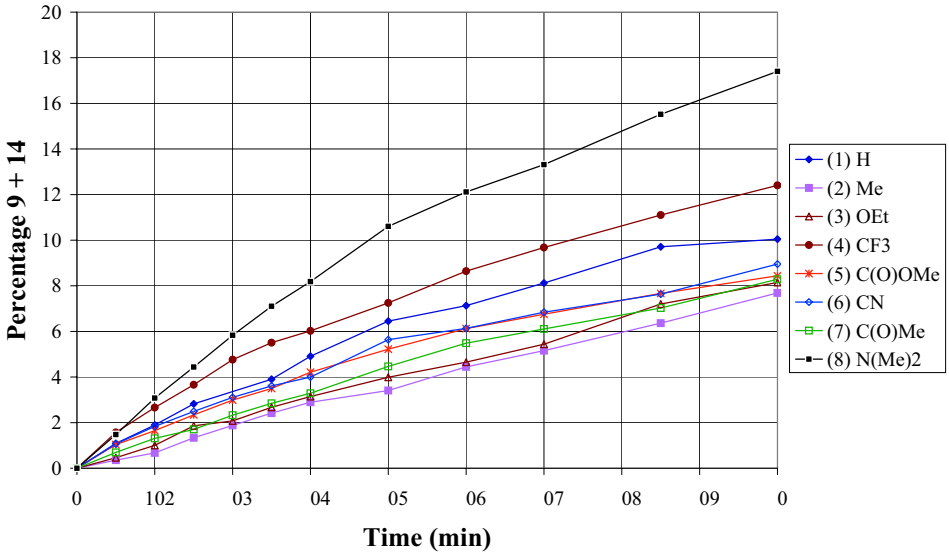

The photoreactivities of both the EDG-substituted **2** and **3** and the EWG-substituted **5**-**7** are similar but all reactions proceed slower than the photolysis of **1**. On the other hand, the EWG-substituted **4** and the EDG-substituted **8** are more photoreactive than **1**. The decreased photoreactivity of **2** and **3** is probably due to the inductive or mesomeric stabilisation of the positive charge on the iodine centre. Likewise, the high photoreactivity of **4** is caused by destabilisation of the iodonium cation by the strongly electron-withdrawing CF_3 group. The EWG-substituents (S = $C(O)OCH_3$, CN, $C(O)CH_3$) in **5**, **6** and **7** also will destabilise the positive charge, but these substituents are known to induce an alternative pathway of deactivation of the excited state leading to non- or less-productive (photon wasting) $n\pi^*$ excited states.

The UV-Vis spectrum of **8**, the most reactive compound, in methanol and acetonitrile (Table S1 in the Experimental Section) shows an absorption maximum at much longer wavelength than the other salts, in solution. This red-shift is probably caused by strong mesomeric delocalisation of the positive charge by the electron-donating $N(Me)_2$ group (Scheme 4). Mesomeric[30] structure **8**-**m** is proposed to contribute to the instability toward light by opening alternative, more efficient, C=I/C-I bond cleavage channels.

Scheme 4: Mesomeric structure of **8**.

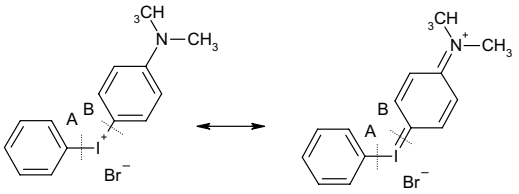

8 mesomer **8-m**

*Photoselectivity in **1**-**8***

The ratios in which the leaving groups **9** and **14** are produced, are indicative of the relative occurrence of A bond cleavage and B bond cleavage in **1**-**8**. These ratios are substituent dependent (Table 3). The EDG-substituted salts **2** and **3** favour A bond cleavage over B bond cleavage, probably because of the increased electron density in the B bond. The EWG-substituted **4** and **5**-**7** act the other way round. The ratio found in the photolysis of **8** does not fit the picture. The expected increase in the bond order of bond B [31] does not bring about a **9** to **14** ratio > 1 as with iodonium salts **2** and **3**. Fission of bond B in **8** presumably is more efficient than in **1** or **2** (See above)

Table 3: The ratio of **9** to **14**.

Salt	S	Ratio
1	H	1.0
2	CH_3	1.5
3	OCH_2CH_3	1.2
4	CF_3	0.8
5	$C(O)OCH_3$	0.7
6	CN	0.4
7	$C(O)CH_3$	0.6
8	$N(CH_3)_2$	0.8

Regioselectivity of product formation

According to the theoretical evaluation, products **15** and **19** are formed via a Friedel-Crafts type recombination of the fragments produced upon either a homolytic or a heterolytic cleavage of the aryl-iodonium bond (B) of the triplet excited state (Scheme 5).

Scheme 5: Possible reactive intermediates, leading to recombination products **15** and **19**.

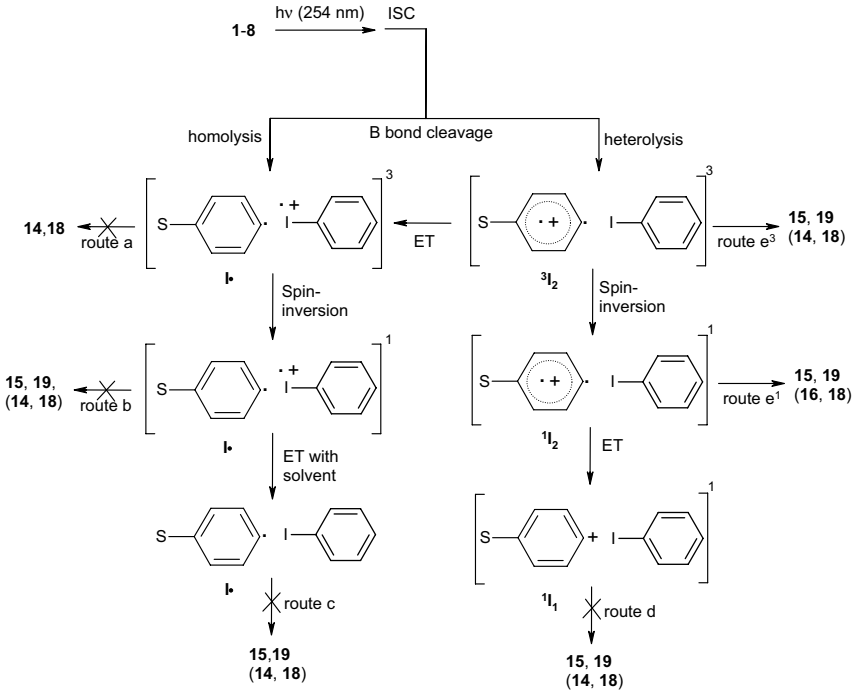

Homolysis gives a phenyl radical-iodobenzene radical cation pair in its triplet state, which also may be formed through heterolysis to the open-shell phenyl cation (^{3}**I**$_2$)-iodobenzene pair followed by electron transfer. This triplet radical pair is less likely to produce recombination products and will preferentially form the leaving group **14** and the reduction product **18** (route a). Radical recombination yielding **15** and **19** (route b) is only possible in the singlet radical pair, which may have formed after spin-inversion. Oxidation of methanol by the iodobenzene radical cation, which produces the phenyl radical (**I**•)-iodobenzene pair, may also lead to re-combination products (route c)[15]. The open-shell phenyl cation ^{3}**I**$_2$, formed upon heterolysis, may convert to its ground state singlet (closed shell) manifold ^{1}**I**$_1$ via spin-inversion to the singlet open-shell cation ^{1}**I**$_2$ followed by intramolecular electron transfer. The phenyl cation (^{1}**I**$_1$)-iodobenzene pair may give rise to the recombination products **15** and **19** (route d), just like its predecessors, the phenyl cation (^{1}**I**$_2$ and ^{3}**I**$_2$) iodobenzene pairs (routes e^1 and e^3). The *o*, *m*, *p* pattern of products **15**, (Table 4), albeit formed in minute amounts with **2**-**8**, sheds light on the actual product-forming intermediate (routes b-e).

Recombination of the singlet phenyl radical-iodobenzene radical cation pair (route b) is expected to take place at the position(s) with highest spin density. According to the PM3-calculated spin-densities in the radical cation of iodobenzene (Scheme 6), the *ipso* and the *para*

Table 4: *O*: *m*: *p* ratios of products **15** obtained after concentration of the reaction mixtures.

	S	15*o*: *m*: *p* ratio
1	H	85:6:9
2	CH_3	79:10:11
3	OCH_2CH_3	87:6:8
4	CF_3	66:6:27
5	$C(O)OCH_3$	72:5:23
6	CN	71:4:35
7	$C(O)CH_3$	66:5:29
8	$N(CH_3)_2$	82:3:15

position would be the preferred sites of attack leading to *ipso*- and *para*- substituted products. Mesomeric structures of the distonic iodobenzene radical cation also indicate that the *ortho* and *para* position possess most of the radical functionality. The thermolysis of diphenyliodonium salts in anisole, which predominantly produces the singlet phenyl radical-iodobenzene radical cation pair, yields products **15** in an *o*, *m*, *p* ratio of 35:11:54 and in 2.6 fold excess over the *ipso* substitution product **19**[32]. The different regio- and chemoselectivity in the thermolysis and the photolysis make route b unlikely for the formation of **15** and **19**.

A phenyl radical-iodobenzene pair[12] can also not be held accountable for the Friedel-Crafts type product pattern (route c). Photolysis of iodobenzene in acetonitrile (4/1) produces a phenyl radical that reacts with iodobenzene itself and yields **15** in an *o*, *m*, *p* ratio of 64:28:8, in 11 fold excess over biphenyl **19**. These data are in agreement with literature data for the radical phenylation of iodobenzene (*o*: *m*: *p* = 55:28:17)[33] but not with the data in Tables 1 and 4.

Scheme 6: PM3-calculated spin densities in and resonance structures of the radical cation of iodobenzene.

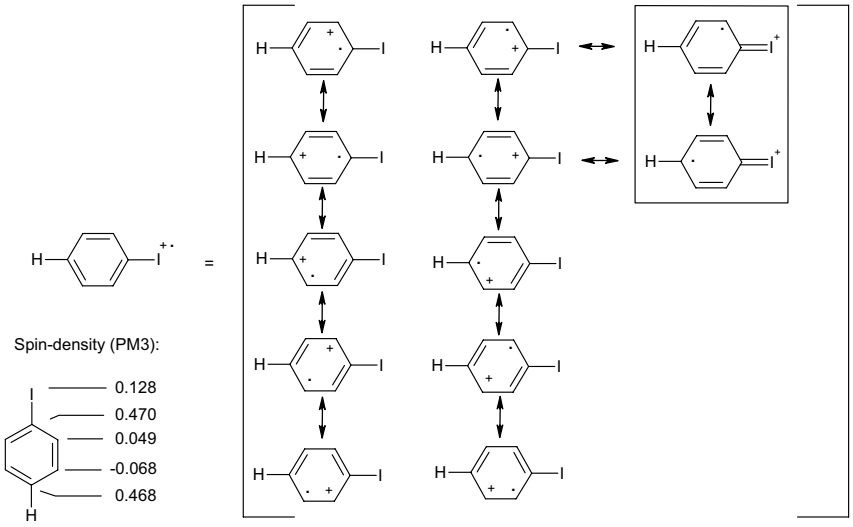

Recombination of the closed shell phenyl cation $^1\mathbf{I}_1$ and iodobenzene (route d) is also not the source of the iodobiphenyl products. The generation of the parent singlet phenyl cation by β-decay of ditritiobenzene in the presence of chlorobenzene yields chlorobiphenyls in an *o*, *m*, *p* ratio of 50:29:21[34]. A similar ratio is expected for the reaction between that cation and iodobenzene. The different *o*, *m*, *p* ratios in which the iodobiphenyls **15** are produced in the photolyses of **1**-**8** (Table 4) and in the β-decay, rule out $^1\mathbf{I}_1$ as product-forming intermediate.

The open-shell cation $^3\mathbf{I}_2$ is a soft Lewis acid and is expected to attack iodobenzene (route e^3) with the regioselectivity of an electrophilic radicaloid species ($o > m > p$, as with **I**•, or with $^1\mathbf{I}_1$) but, contrary to these intermediates, also with a preference for polarisable (soft Lewis

Scheme 7: Mechanism of formation of **15** and **19**.

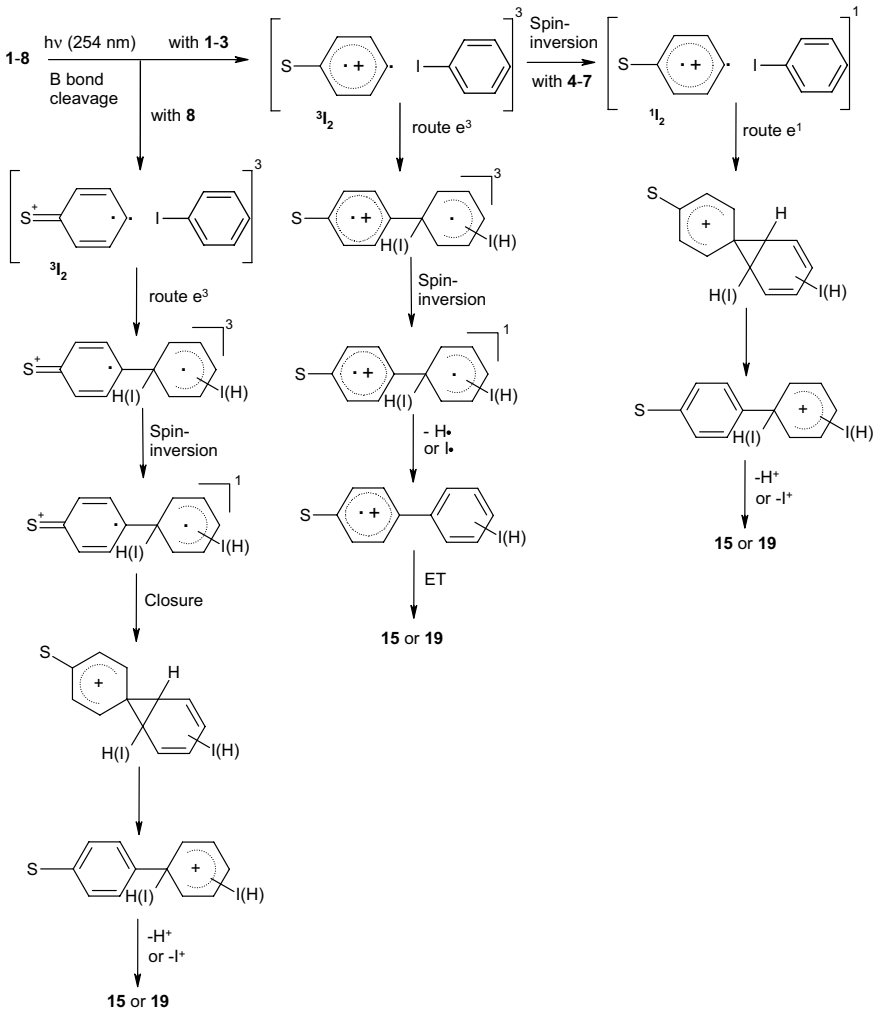

base) positions (*i* > *o* >> *m*, *p*). The cations formed upon irradiation of **1**-**3** (S = H, CH_3 and OCH_2CH_3) react with iodobenzene to produce mainly *ipso* and *ortho* diradical cation addition complexes (Scheme 7). After spin-inversion and loss of a hydrogen atom or an iodine atom **15** and **19** are produced. The *o*, *m*, *p* ratios of **15** produced upon photolysis of **1**-**3** (Table 4) indicate the cations to be of triplet nature ($^3\mathbf{I}_2$).

The higher percentage of the *para* isomer in product **15** in the irradiation of **8** is caused by the strong mesomeric electron-donating effect of the $N(CH_3)_2$ group. Upon formation of the initial addition complex and spin-inversion, the delocalisation of the positive charge onto the nitrogen substituent, grants a cationic spiro-compound to form (Scheme 7). In turn, the spiro-compound opens to the more stable Wheland-intermediate (*o*, *p* > *m*). Upon cleaving off I^+ or H^+, **19** and **15** are produced. This pathway allows conversion of the initial *meta* distonic diradical cation into either the *ortho* or the *para* Wheland-intermediate, which causes an increase in *para* and a depletion in *meta* product **15**.

The electron withdrawing substituents in **4**-**7** (S = CF_3, $C(O)OCH_3$, CN and $C(O)CH_3$) destabilise $^3\mathbf{I}_2$. Therefore a swift isomerisation to $^1\mathbf{I}_2$ (and further to $^1\mathbf{I}_1$) is expected. The open-shell cation $^1\mathbf{I}_2$ is expected to attack iodobenzene with the regioselectivity of a singlet carbene (route e^1) which directly yields the cationic spiro-compounds with a preference *i*, *o* > *o*, *m* and *m*, *p* (Scheme 7). Opening of the spiro-compounds to the more stable Wheland intermediate (*o*, *p* > *m*) and subsequent expulsion of I^+ or H^+ produces **19** and **15**. The *o*: *m*: *p* ratios of **15** produced upon photolysis of **4**-**7** (Table 4) substantiate the intermediacy of $^1\mathbf{I}_2$.

The formation of **10**, which occurs through A bond cleavage, only takes place in the photolyses of **2** and **3**. The isomeric distribution between **10a** and **10b** is caused by the balance of radical stabilizing effects of the two substituents at the substrate that govern the position of attack of the radicaloid electrophilic triplet phenyl cation. The non-formation of product **10** in the photolyses of **4**-**7** is caused by the double electron-withdrawing substituted aromatic fragment being less activated for electrophilic attack than the CH_3- and OCH_2CH_3-substituted fragments. The lack of formation of **10** in the photolysis of **8** is attributed to trapping of the product-forming intermediate by the counter-ion Br^- instead of by the iodoaromatic fragment. These arguments also explain why less **19** is formed in the photolyses of **5**-**8** than in the photolyses of **1**-**3**. The unexpectedly large percentage of **19** in the photolysis of **4** is due to the relatively high conversion in this photoreaction.

Chemoselectivity

Nucleophilic substitution with the solvent, yielding the methyl ethers **11** and **16**, is the result of the attack of the phenyl cation intermediate $^1\mathbf{I}_1$, a hard Lewis acid, at the n-electrons of methanol[15], a hard Lewis base. Subsequent loss of a proton gives the methyl ether products (as to the

counter-ion, no Schiemann product of the parent phenyl cation with BF_4^- is observed under the reaction conditions). The reaction is a major product-forming route upon A bond cleavage of the iodonium salts under study (Table 5, column 3). Only in the case of the OCH_2CH_3- and $N(CH_3)_2$ substituted salts **3** and **8**, its role is diminished. Upon B bond fission, only in the photolysis of **1** and **2**, and much less so in **3** and **4**, reactions occur of the phenyl cation $^1\mathbf{I}_1$ with the solvent, leading to **16**.

Table 5: Formation of ethers **11** and **16** and reduction products **13** and **18** (relative to the formation of the leaving group in the cleavage leading to that product).

	S	11	16	13	18
1	H	0.33	0.33	0.28	0.28
2	CH_3	0.25	0.37	0.25	0.28
3	OCH_2CH_3	0.14	0.06	0.25	0.48
4	CF_3	0.27	0.06	0.22	0.67
5	$C(O)OCH_3$	0.5		0.34	0.67
6	CN	0.81		0.48	0.75
7	$C(O)CH_3$	0.63		0.56	0.44
8	$N(CH_3)_2$	0.04		0.43	0.14

Reduction, yielding **13** and **18**, is the result of hydrogen atom abstraction from the solvent by a phenyl radical intermediate **I•**, formed after homolysis from the triplet excited state. Unlike the nucleophilic substitution products, the reduction products **13** and **18** are found in all experiments (Table 5). An alternative route for the formation of the reduction products **13** and **18** is through the triplet (open-shell) phenyl cations. These ions may abstract a hydrogen atom from the solvent and produce radical cations, which upon electron transfer give **13** or **18**.

The bromides **12** and **17** in the photolysis of **8** (Table 1) are produced by trapping of the phenyl cations by the bromide anion. Cation $^3\mathbf{I}_2$, a soft Lewis acid, is expected to be trapped more efficiently by the bromide anion, a soft Lewis base, than the closed shell cation $^1\mathbf{I}_1$ (HSAB principle). The formation of **12** and **17** therefore is attributed to the intermediacy of the triplet phenyl cations $^3\mathbf{I}_2$ generated upon A and B bond cleavage.

*Regio- and chemoselectivity of **1**-**8** in acetonitrile/anisole*

Comparison of the product patterns in Table 2 with those of the phenyl cation and the phenyl radical under similar reaction conditions reveal the nature of the product-forming intermediate. The β-decay of 1,4-ditritiobenzene, which forms the singlet phenyl cation $^1\mathbf{I}_1$, in anisole, produces **20** in an *o*, *m*, *p* ratio of 65:13:22[34]. The amount of reduction product could not be determined because monotritiobenzene can not be distinguished from ditritiobenzene.

The photolysis of iodobenzene, which produces the phenyl radical, in acetonitrile/anisole yields products **20** in an *o*, *m*, *p* ratio of 75:13:12 and in a 2.1 fold excess over the reduction product **13**.

The *o*, *m*, *p* ratios of **20** collected in column 11 of Table 2, except for **8**, all are similar to the ratio observed in the literature for the singlet phenyl cation, which indicates $^1\mathbf{I}_1$ as product-forming intermediate in Scheme 3. The slightly higher percentages of **20**-*ortho* and lower percentages of **20**-*para* in the photolysis of **1**, **2** and **4** may be due to a contribution of a phenyl radical route to the formation of **20**.

The *o*, *m*, *p* ratios observed for biaryls **21** in the photolysis of **1**-**7** (Table 2, column 12) show similarity with the ratio typical for the singlet phenyl cation (65:13:22) and with the ratio typical for the phenyl radical (75:12:13). However, the excess of arylation over reduction with **1**-**7**, indicates that the radical pathway is not a major product-forming route. It does contribute to some extent in the photoreactions of **2** and **3**.

The *o*, *m*, *p* ratios found for products **21** are attributed to the combined reactivity of the closed shell phenyl cations ($^1\mathbf{I}_1$) and the triplet phenyl cations ($^3\mathbf{I}_2$). Triplet phenyl cations substituted with an EWG, prepared photochemically from the corresponding diazonium compounds, are also found to give products with *o*, *m*, *p* ratio characteristic of a phenyl radical, and to preferentially arylate an aromatic substrate over abstracting a hydrogen atom from the solvent (See Chapter 4).

In the photolysis of **8** only a small (A: 1.8, B: 1.5 fold) excess of arylation over reduction is observed. The production of **20*o***, ***m***, ***p*** in a ratio typical for a phenyl radical intermediate and the selective formation of **21*o***, which is also observed in the photolysis of iodobenzene in anisole at very low conversion, indicate that the formation of **13**, **18**, **20** and **21** from **8** largely takes place through a phenyl radical intermediate.

This certainly does not mean that no phenyl cation is produced upon irradiation of **8**. If formed, the open-shell phenyl cation is trapped more efficiently by the counter-ion bromide than by anisole. The contribution of the photohomolysis now becomes visible through its distinct product pattern of aromatic substitution and hydrogen atom abstraction.

Conclusions

The regio- and chemoselectivities observed in the photoreactions of the iodonium salts **1**-**8** lead to the proposal for the mechanism of the photolysis of diphenyliodonium salts depicted in Scheme 8. The C-I$^+$ bond cleavages proceed from the triplet excited state. The bond fission occurs mainly heterolytically, yielding the open-shell aryl cations $^3\mathbf{I}_2$. Intermediates **I•** generated

through homolysis, or through electron transfer from $^3\mathbf{I}_2$, play a minor role. This proposal is supported by the results of the theoretical evaluation of the bond cleavage reactions.

Scheme 8: Proposed mechanism of photolysis of diphenyliodonium salts.

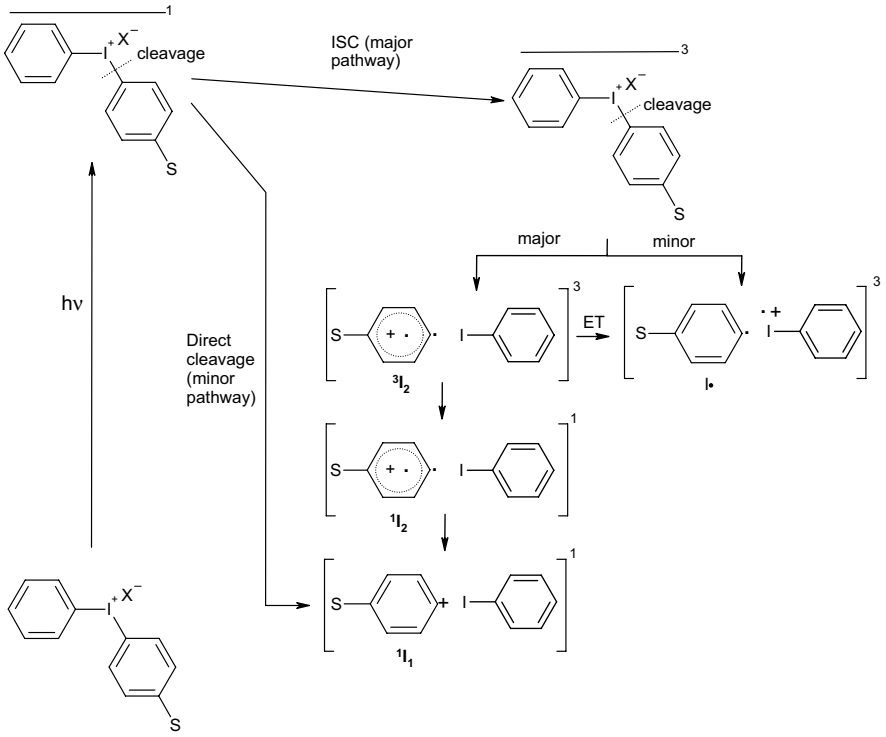

If $^3\mathbf{I}_2$ is destabilised by an EWG, the triplet to singlet cation conversion is faster than trapping by the internal nucleophiles iodobenzene or bromide anion. In that case the $^3\mathbf{I}_2$ state is trapped by the internal π nucleophile iodobenzene. Further isomerisation leads to $^1\mathbf{I}_1$ which may be trapped by external nucleophiles such as methanol.

In the presence of the external n- and π-nucleophile anisole an almost uniform product pattern is found in all irradiations. The time necessary for the $^3\mathbf{I}_2$ intermediates formed in the irradiation of **1**-**7**, to react with anisole, is enough to almost completely isomerise to their $^1\mathbf{I}_1$ ground state and react as such. The cation $^3\mathbf{I}_2$ formed in the photolysis of **8** is the ground state.

Experimental Section

Materials

All solvents are distilled prior to their use in synthesis. The iodonium salts **1**-**4** and **6**,**7** are synthesised from the corresponding, commercially available, 4-substituted phenyl boronic acids, according to an altered literature procedure[21,22]. 1.61 g of (diacetoxyiodo)benzene (5 mmol) is suspended in 40 mL dichloromethane. The white suspension is cooled to -30°C in a dry ice/ acetone bath and 1.63 mL of 54% w/w HBF_4 in diethyl ether (10 mmol) is added drop by drop. A yellow solution is formed. After stirring for 30 minutes the reaction mixture is cooled to -30°C and the *para*-substituted phenyl boronic acid (5 mmol) is added. The mixture is stirred until all boronic acid has dissolved. If after two hours of stirring still some phenyl boronic acid is left, the mixture is filtered. The reaction mixture is dried with $MgSO_4$. Most of the dichloromethane is evaporated until about 5 mL solution is left. Diethyl ether is added dropwise which causes the raw product to precipitate. The white crystals are filtered and washed with diethyl ether. The products are crystallised three times from dichloromethane/ ether. Yields ± 80%. NMR (^{1}H, $CDCl_3$, 300 MHz): **1**: 7.50-7.56 (t, 4H); 7.66-7.72 (t, 2H); 8.15-8.19 (d, 4H). IR (neat, cm^{-1}): 447, 458 (C-I $^+$)[35], 521, 647-682-746 (peaks characteristic of diphenyliodonium salts), 1020 (broad, peak BF_4^-), 3090. **2**: NMR (^{1}H, $CDCl_3$, 300 MHz) 2.40 (s, 3H); 7.32-7.36 (d, 2H); 7.48-7.54 (t, 2H); 7.64-7.70 (t, 1H); 8.01-8.05 (d, 2H); 8.11-8.15 (d, 2H). IR (neat, cm $^{-1}$): 448, 479, 522, 650-676-744, 1020, 3090. **3**: NMR (^{1}H, CD_3OH 300 MHz) 1.35-1.41 (t, 3H); 3.96-4.04 (q, 2H); 6.88-6.92 (d, 2H); 7.37-7.43 (t, 2H); 7.51-7.57 (t, 1H); 7.93-7.98 (d, 4H). IR (neat, cm^{-1}): 454, 508, 520, 654-678-739, 1020, 1256 (C-O), 2983, 3099. **4**: NMR (^{1}H, CD_3OH, 300 MHz) 7.53 (t, 2H); 7.69-7.75 (t, 1H); 7.79-7.83 (d, 2H); 8.21-8.24 (d, 2H); 8.34-8.38 (d, 2H). IR (neat, cm^{-1}): 452, 493, 524, 654-678-746, 1020, 1322 (C-F), 1400, 3099. **6**: NMR (^{1}H, CD_3OH, 300 MHz) 7.53-7.59 (t, 2H); 7.70-7.76 (t, 1H); 7.84-7.88 (d, 2H); 8.19-8.23 (d, 2H); 8.30-8.34 (d, 2H). IR (neat, cm^{1}): 457, 521, 543, 654-680-750, 1020, 2248 (C≡N), 3093. **7**: NMR (^{1}H, CD_3OH, 300 MHz) 2.61 (s, 3H); 7.52-7.58 (t, 2H); 7.68-7.74 (t, 1H); 8.04-8.08 (d, 2H); 8.19-8.22 (d, 2H); 8.27-8.30(d, 2H). IR (neat, cm^{-1}): 459, 522, 654-683-714, 1020, 1670 (C=O), 3090.

In order to synthesise **5,** 4-iodobenzoic acid is esterified to 4-iodobenzoic acid methyl ester according to a literature procedure[36]. This ester is oxidised to 4-iodobenzoic acid methyl ester diacetate[37]. From this compound **5** is synthesised by reacting it with phenyl boronic acid using the procedure described above. Yield = 75%. NMR (^{1}H, CD_3OH, 300 MHz): **5** 4.02 (s, 3H); 7.61-7.68 (t, 2H); 7.78-7.84 (t, 1H); 8.17-8.21 (d, 2H); 8.26-8.30 (d, 2H); 8.33-8.37 (d, 2H). IR (neat, cm^{-1}): 448, 471, 519, 652-679-748, 1020, 1303 (C-O), 1704 (C=O), 2950, 3090.

Iodonium salt **8** is synthesised from 4-N,N-dimethylaminobenzeneboronic acid (5 mmol) en hydroxy(tosyloxy) iodobenzene (Koser's reagent) (5 mmol) in THF. The reaction mixture is stirred for 90 min at 0°C. Evaporation of THF leaves a green product: the tosylate salt of **8**. This product is dissolved in dichloromethane and the solution is washed three times with a satu -

rated KBr solution in water. The organic layer is dried with $MgSO_4$ and evaporated. Crystallisation from dichloromethane/pentane for three times yields green powderish bromide salt **8** in 28%. NMR (^1H, CD_3OH, 300 MHz): 3.03 (s, 6H); 6.72-6.79 (d, 2H) 7.45-7.52 (t, 2H); 7.60-7.66 (t, 1H); 7.86-7.92 (d, 2H); 8.00-8.04 (d, 2H). IR (neat, cm^{-1}): 456, 502, 652- 682-746, 1063 cm^{-1} (C-N), 1599 cm^{-1} (C=C), 2850 cm^{-1}, (C-H); 3090 cm^{-1}.

Table S1: UV-Vis spectra of **1**-**8** in methanol and acetonitrile (λ in nm, ε in $M^{-1}cm^{-1}$).

	S	$\lambda_{max, MeOH}$	ε_{max}#	ε_{254}#	$\lambda_{max, ACN}$	ε_{max}#	ε_{254}#
1	H	225.9	$2.56*10^4$	$4.21*10^3$	229.1	$2.02*10^4$	$9.10*10^3$
2	CH_3	244.9	$2.61*10^4$	$2.12*10^4$	250.0	$1.74*10^4$	$1.68*10^4$
3	OCH_2CH_3	247.0	$1.82*10^4$	$1.56*10^4$	251.1	$1.55*10^4$	$1.52*10^4$
4	CF_3	226.0	$1.75*10^4$	$1.76*10^3$	226.0	$2.14*10^4$	$8.52*10^3$
5	$C(O)OCH_3$	236.0	$1.83*10^4$	$6.68*10^3$	238.0	$2.60*10^4$	$6.68*10^3$
6	CN	236.9	$3.17*10^4$	$9.61*10^3$	239.0	$2.93*10^4$	$1.54*10^4$
7	$C(O)CH_3$	244.0	$3.36*10^4$	$2.35*10^4$	244.0	$0.27*10^4$	$2.09*10^4$
8	$N(Me)_2$	304.0	$2.03*10^4$	$1.37*10^4$	311.1	$1.70*10^3$	$1.95*10^4$

ε_{max} is absorption coefficient at maximum absorption, ε_{254} is absorption coefficient at λ = 254 nm.

Photochemistry

The photochemical reactions in methanol were carried out in quartz tubes equipped with a rubber seal, that are placed in a merry-go-round apparatus. A Hanau TNN-15/32 low pressure mercury lamp placed in a water cooled quartz tube is used to supply light with a main emission at λ = 254 nm. For the irradiations 0.02 M solutions of the iodonium salts **1**-**8** in 10 mL methanol are prepared. 25 µL n-decane is added as internal standard. Samples (200 µl) are taken at t = 0, 5, 10, 15, 20, 25, 30, 40, 50, 60, 70 and 90 minutes of irradiation. Up till that time the conversions are still low and all products are primary products. The samples are added to 500 µL water and 300 µL ethylacetate. The organic layers are analysed by GC and GC-MS. The 90 minutes irradiation mixtures are poured in 50 mL water and extracted with 10 mL ethylacetate. The organic layer is separated and dried with $MgSO_4$. The solvent is evaporated and the residues were redissolved in 0.5 mL dichloromethane for GC and GC-MS analysis.

The photochemical reactions in acetonitrile/anisole were carried out in quartz tubes equipped with a rubber seal. The starting materials were dissolved at 0.02 M in 10 mL 1/1 acetonitrile/anisole. 25 µL *n*-Decane was used as internal standard. The tubes were placed in a Rayonet Reactor (RPR200) fitted with seven 254 nm lamps and stirred. The photolyses of the salts **1**-**8** were followed as a function of time by taking aliquots (0.2 mL sample) and adding them to 0.5 mL water + 0.3 mL ethylacetate. The organic layers were analyzed by GC and GC-MS.

Photoproducts

The assignment of the structures by GC and GC-MS was confirmed by coinjection of commercially available or independently prepared products. Products **9**, **11**, **12**, **13**, **14**, **16**, **17**, **18** and **20*o*, *m*, *p*** are commercially available. Products **10a**-CH_3/**10b**-CH_3 and **10a**-OCH_2CH_3/**10b**- OCH_2CH_3 are prepared by reacting benzenediazonium tetrafluoroborate with **9**-CH_3 and **9**-OCH_2CH_3 in acetonitrile. The reaction mixtures were diluted with ethylacetate and used as such for coinjection. The Friedel-Crafts products **15**-H are prepared by reacting benzenediazonium tetrafluoroborate with iodobenzene in acetonitrile (1/1). The ethylacetate-diluted product mixture is used for coinjection. The structures of all other products **15** (Table 4) are assigned tentatively. The *ipso*-substitution products **19** were prepared photochemically from either **9** or **17** and benzene, dissolved in acetonitrile (1/1) at λ_{exc} = 254 nm in a RPR200 Rayonet reactor. The irradiation mixtures were poured in water and extracted with ethylacetate. Products **21** are prepared photochemically by reacting **9** with anisole dissolved in acetonitrile under the same reaction conditions as used for **19**.

Equipment

UV spectra were recorded at room temperature on a double beam Varian DMS 200 Spectrophotometer, if applicable with pure solvent in the reference cell. ^{1}H-NMR spectra were recorded on a DMX 300, using DMSO D_6 as solvent. As analytical GC a Hewlett-Packard 6890 model was used, equipped with a automatic injector, fitted with a CP-Sil5-CB column (25 m, ø = 0.25 mm, 1.2 µm) using hydrogen as carrier gas. The Flame-Ionisation Detector (FID) was calibrated using commercially available reference chemicals. HP Chemstation was used for the analysis of the analytical data. Mass spectra were measured on a GC-MS set-up consisting of a Hewlett-Packard 5890 series 2 model GC, equipped with a automatic injector, fitted with a AT-5MS column (30 m, ø = 0.25 mm, 0.25 µm) using helium as carrier gas. The GC was coupled to a Finnigan Mat SSQ 710 mass spectrometer, employing electron-impact as the ionisation method. The GC-MS data was analyzed with Xcaliber.

References and Notes

[1] Hartmann, C.; Meyer, V. *Chem. Ber.* **1894**, *27*, 426-432.

[2] Willgerodt, C. *J. Prakt. Chem.* **1886**, *33*, 154-160.

[3] a) Willgerodt, C. *Die Organischen Verbindingen mit Mehrwertigem Jod*, F. Enke, Stuttgart: **1914**. Beringer, F. M.; Gindler, E. M. *Iodine Abstr. Rev.* **1956**, 3. b) Banks, D. F. *Chem. Rev.* **1966**, 66, 243-266. c) Koser, G.F. in *The Chemistry of Functional Groups, Supplement D*, Patai, S.; Rappoport, Z., Eds., John Wiley & Sons, New York: **1983**, part 1, chap 18. d) Varvoglis, A. in *Topics in Current Chemistry 224*, Wirth, T. Ed. Springer-Verlag: Heidelberg-Berlin: **2003**, pp 69-98.

[4] a) Hwang, W. K. *Chem. Abstr.* **1957**, *51*, 16476. b) Hwang, W. K.; Wang, C. H.; Chen, S. Y. *Chem. Abstr.* **1957**, *53*, 4280. c) Irving, H.; Reid, R. W. *J. Chem. Soc.* **1960**, 2078-2081.

[5] a) Levit, A. F.; Korosryshevskii, I. Z.; Gragerov, I. P. *Zh. Org. Khim.* **1970**, *6*, 1878-1882. b) McEwen, W. E.; De-Massa, J. W. *Heteroatom Chem.* **1996**, *7*, 349-354.

[6] a) Crivello, J. V.; Lam, J. H. W. *Macromolecules* **1977**, *10*, 1307-1315. b) Crivello, J. V. *Adv. Polym. Sc.* **1984**, *62*, 1-47. c) Crivello, J.V. In *Radiation Curing In Polymer Science and Technology*; Fouassier, J. P., Rabek, J. F., Chapman & Hall: Londen, **1993**; Vol. 2, pp 435-471. d) Helbert, J. N.; Daou, Y. in *Handbook of VLSI Microlithography*, J. N. Helbert Ed., William Andrew Publishing LLC, Norwich, NY: 2001, pp. 75-314.

[7] DeVoe, R. J.; Olofson, P. M.; Sahyun, M. R. V. *Adv. Photochem.* **1992**, *17*, 313-355.

[8] a) Knapczyk, J. W.; McEwen, W. E. *J. Org. Chem.* **1970**, *35*, 2539-2543. b) Dektar, J. L.; Hacker, N. P. *J. Org. Chem.* **1988**, *53*, 1835-1837. c) Dektar, J. L.; Hacker, N. P. *J. Am. Chem. Chem.* **1990**, *112*, 6004-6015. d) Welsch, K. M.; Dektar, J. L.; Garcia-Garibaya, M. A.; Hacker, N. P.; Turro, N. J. *J. Org. Chem.* **1992**, *57*, 4179-4184.

[9] Ohmori, N.; Nakazono, Y.; Hata, M.; Hoshino, T.; Tsuda, M. *J. Phys. Chem. B* **1998**, *102*, 927-930.

[10] Knapczyk, J. W.; Lubinkowski, J. J.; McEwen, W. E. *Tetrahedron Lett.* **1972**, 3789.

[11] Klemm, E.; Riesenberg, E.; Graness, A. *Z. Chem.* **1983**, *23*, 222.

[12] a) Pappas, S. P.; Jilek, J. H. *Photogr. Sci. Eng.* **1979**, *23*, 140. b) Pappas, S. P.; Pappas, B. C.; Gatechair, L. R.; Schnabel, W. *J. Polym. Sci., Polym. Chem. Ed.* **1984**, *22*, 69-76. c) Pappas, S. P.; Gatechair, L. R.; Jilek, J. H. *J. Polym. Sci., Polym. Chem. Ed.* **1984**, *22*, 77-84. d) Pappas, S. P.; Pappas, B. C.; Gatechair, L. R.; Jilek, J. H.; Schnabel, W. *Polym. Photochem.* **1984**, *5*, 1-22.

[13] Devoe, R. J.; Sahyun, M. R. V.; Serpone, N.; Sharma, D. K. *Can. J. Chem.* **1987**, *65*, 2342-2349.

[14] Timpe, H. J.; Schikowsky, V. *J. Prakt. Chem.* **1989**, *331*, 447-460.

[15] a) Dektar, J. L.; Hacker, N. P. *J. Org. Chem.* **1990**, *55*, 639-647. b) Dektar, J. L.; Hacker, N. P. *J. Org. Chem.* **1991**, *56*, 1838-1844. c) Hacker, N. P.; Leff, D. V.; Dektar, J. L. *J. Org. Chem.* **1991**, *56*, 2280-2282.

[16] Kitamura, T. in *CRC Handbook of Organic Photochemistry and Photobiology, 2nd edition* Horspool, W. M.; Lenci, F. Eds., CRC Press LLC: Boca Raton **2004**, Chapter 110.

[17] a) Neikam, W. C.; Dimeler, G. R.; Desmond, M. M. *J. Electrochem. Soc.* **1964**, *111*, 1190. b) Fisher, I. P.; Palmer, T. F.; Lossing, F. P. *J. Am. Chem. Soc.* **1964**, *86*, 2741-2742. c) Miller, L. L.; Nordblom, G. D.; Mayeda, E. A. *J. Org. Chem.* **1972**, *37*, 916-918. d) Butcher, V.; Costa, M. L.; Dyke, J. M.; Ellis, A. R.; Morris, A. *Chem. Phys.* **1987**, *115*, 261-262. e) Baidan, V. N.; Misharev, A. D.; Takhistov, V. V. *Zh. Org. Khim.* **1985**, *21*, 817-822.

[18] *Dicoordinated Carbocations*; Rappoport, Z.; Stang, P., Eds.; John Wiley & Sons Ltd.: Chichester, UK, **1997**.

[19] a) Gaspar, S. M.; Devadoss, C.; Schuster, G. B. *J. Am. Chem. Soc.* **1995**, *117*, 5206-5211. b) Vrkic, A. K.; O'Hair, A. J. *Int. J. Mass Spectrom.* **2002**, *218*, 131-160 c) Canning, P. S. J.; Maskill, H.; McCrudden, K.; Sexton, B. *Bull. Chem. Soc. Jpn.* **2002**, *75*, 789-800.

[20] a) Guizzardi, B.; Mella, M.; Fagnoni, M.; Freccero, M.; Albini, A. *J. Org. Chem.* **2001**, *66*, 6353-6363. b) Protti, S.; Fagnoni, M.; Mella, M.; Albini, A. *J. Org. Chem.* **2004**, *69*, 3465-3473. c) Milanesi, S.; Fagnoni, M.; Albini, A. *J. Org. Chem.* **2005**, *70*, 603-610.

[21] Ochiai, M.; Toyonari, M. Nagaoka, T.; Chen, D-W.; Kida, M. *Tetrahedron Lett.* **1997**, *38*, 6709-6712.

[22] Caroll, M. A.; Pike, V. W.; Widdowson, D. A. *Tetrahedron Lett.* **2000**, *41*, 5393-5396.

[23] Michl, J.; Bonačić-Koutecký, V. B. *Electronic Aspects of Organic Photochemistry*, VCH Publishers, Inc., New York: 1995, Chapter 6, pp. 318-319.

[24] Gaussian 98, Revision A.9, Frisch, M. J.; Trucks, G. W.; Schlegel, H. B.; Scuseria, G. E.; Robb, M. A.; Cheese - man, J. R.; Zakrzewski, V. G.; Montgomery, J. A.; Stratmann, R. E.; Burant, J. C.; Dapprich, S.; Millam, J. M.; Daniels, A. D.; Kudin, K. N.; Strain, M. C.; Farkas, O.; Tomasi, J.; Barone, V.; Cossi, M.; Cammi, R.; Mennucci, B.; Pomelli, C.; Adamo, C.; Clifford, S.; Ochterski, J.; Petersson, G. A.; Ayala, P. Y.; Cui, Q.; Morokuma, K.; Malick, D. K.; Rabuck, A. D.; Raghavachari, K.; Foresman, J. B.; Cioslowski, J.; Ortiz, J. V.; Baboul, A. G.; Stefanov, B. B.; Liu, G.; Liashenko, A.; Piskorz, P.; Komaromi, I.; Gomperts, R.; Martin, R. L.; Fox, D. J.; Keith, T.; Al-Laham, M. A.; Peng, C. Y.; Nanayakkara, A.; Gonzalez, C.; Challacombe, M.; Gill, P. M. W.; Johnson, B.; Chen, W.; Wong, M. W.; Andres, J. L.; Gonzalez, C.; Head-Gordon, M.; Replogle, E. S.; and Pople, J. A., Gaussian, Inc., Pittsburgh, USA, 1998.

[25] Gilbert, A.; Baggott, J. *Essentials in Molecular Photochemistry*, Blackwell Scientific Publications: Oxford **1991**, Chapter 3, p 81.

[26] Gilbert, A.; Baggott, J. *Essentials in Molecular Photochemistry*, Blackwell Scientific Publications: Oxford **1991**, Chapter 7, pp 287-353.

[27] Milanesi, S.; Fagnoni, M.; Albini, A. *J. Org. Chem.* **2005**, *70*, 603-610.

[28] Complete absorption of light by compounds **1**-**8** was ensured. The quantum yield of formation of the com - bined iodophenyl products is 0.400 at λ_{exc}= 248 nm in acetonitrile [Ref 15a].

[29] a)Yamada, Y.; Okawara, M. *Bull. Chem. Soc. Jpn.* **1972**, *45*, 2515-2519. b) Yamada, Y.; Kashima, K.; Okawara, M. *Bull. Chem. Soc. Jpn.* **1974**, *47*, 3179-3180

[30] I am not sure whether**8**-**m** is a mesomer or an isomer of**8**. Crystal structures of phenyliodonium salts indicate an actual bond between iodine and the counter-ion, a structure often referred to as λ^3 iodane [Ochiai, M. in *Top. Curr. Chem. 224*, Wirth, T. Ed. Springer-Verlag: Heidelberg-Berlin:**2003**, p. 7]. The UV-Vis spectrum of **8** suggests a large delocalisation of the positive charge. If (near) complete transfer of the positive charge to nitrogen is achieved and the shift is accompanied by a reorientation of the counter-ion to near the nitrogen atom, the resulting structure is formally an isomer of **8**. Such a structure is reminiscent of that of iodonium ylides which are calculated to possess significant double bond character [a) Moriarty, R. M.; Bailey, B. R.; Prakash, O.; Prakash, I. *J. Am. Chem. Soc.* **1985**, *107*, 1375-1378 b) Camacho, M. B.; Clark, A. E.; Liebrecht, T. A.; DeLuca, J. P. *J. Am. Chem. Soc.***2000**, *122*, 5210-5211 c) Krimse, W. *Eur. J. Org. Chem* **2005**, 237-260]. Since no accurate structural data on (molecules like) **8** are available and complete reorientation of the counter-ion is not proven, the term mesomer is maintained.

[31] Pankratov, A. N. *J. Anal. Chem.* **2005**, *60*, 130-136.

[32] McEwen, W. E.; DeMassa, J. W. *Heteroatom Chem.* **1996**, *7*, 349-354.

[33] a) Augood, D. R.; Cadogan, J. I. G.; Hey, D. H.; Williams, G. H. *J. Chem. Soc.* **1953**, 3412-3417. b) Dannley, R. L.; Gregg, E. C.; Phelps, R. E.; Coleman, C. B. *J. Am. Chem. Soc.* **1954**, *76*, 445-448.

[34] Angelini, G.; Keheyan, Y.; Speranza, M. *Helv. Chim. Act* **1988**, *71*, 107-119.

[35] Bell, R.; Morgan, K. J. *J. Chem. Soc.B* **1960**, 1209-1214.

[36] Kato, Y.; Morgan Conn, M.; Rebek, J. *J. Am. Chem. Soc.* **1994**, *116*, 3279-3284.

[37] Kaźmierczak, P.; Skulski, L. *Synthesis* **1995**, 1027-1032.